

Many-body theory of energy relaxation in an excited-electron gas via optical-phonon emission

S. Das Sarma, J. K. Jain, and R. Jalabert

*Department of Physics, University of Maryland, College Park, Maryland 20742-4111
and Joint Program for Advanced Electronic Materials, Laboratory of Physical Science,
University of Maryland, College Park, Maryland 20742-4111*

(Received 19 June 1989)

We consider relaxation of a hot-electron gas by emission of LO phonons in quasiequilibrium when both the electrons and the lattice are in separate internal equilibria, and the electron distribution function can be described by an effective temperature. We find that, in addition to dynamical screening and the hot-phonon effect, the many-body renormalization of the LO phonons also plays a crucial role, both qualitatively and quantitatively, in the power-loss process at low electron temperatures. The density of states of a LO phonon coupled to an electron gas has three branches: (i) the bare-phonon-like branch near the bare-phonon energy, (ii) the plasmonlike branch near the plasmon energy, and (iii) the low-energy quasiparticle-excitation-like branch in the quasiparticle-excitation region. We show that even though the oscillator strengths of the plasmonlike and the quasiparticle-excitation-like branches are extremely small, they dominate the power-loss process at low enough electron temperatures. This produces an enhancement of the power loss at low electron temperatures by many orders of magnitude relative to the power loss to bare unrenormalized LO phonons. We believe that the hot-electron relaxation experiments are a very suitable way of studying the novel quasiparticle-like LO phonons, which are unlikely to be observed directly because of their small oscillator strength. We provide a detailed quantitative theory for hot-electron relaxation in both two- and three-dimensional systems based on this many-body approach and find quantitative agreement with existing experimental results in the 20–200-K electron-temperature regime.

I. INTRODUCTION

Substantial electron heating occurs in small semiconductor devices due to the presence of large electric fields. Electrons can also be excited optically by the application of a laser pulse. A large amount of experimental and theoretical effort has been invested in recent years to investigate how these electrons relax by losing their energy to the lattice.^{1–3}

There are two important time scales in the problem: the electron equilibration time τ_e , and the electron-phonon scattering time τ_{in} . τ_e corresponds to electrons scattering with (immobile) impurities and electron-electron scattering, which brings about a redistribution of the energy and momentum of the electrons and take the electron gas towards an equilibrium spherical distribution although the electron gas as a whole does not lose energy during these scattering processes. τ_{in} , on the other hand, corresponds to inelastic scattering with phonons in which the electron gas actually loses energy to lattice excitations. When $\tau_e \ll \tau_{in}$, one can make the adiabatic approximation in which the electron gas can be assumed to be in *internal* equilibrium during the entire energy-loss process. Determination of the electronic equilibrium distribution function can, in general, be a rather formidable problem and has recently attracted a great deal of attention, but a substantial amount of progress can be made by assuming that the distribution of the hot electrons is thermal (i.e., it can be described by a Fermi-Dirac distribution function with an effective temperature) because this allows one to exploit the rather well-developed techniques of the finite-temperature field theory. This is usually referred to as the electron “temperature model.”

We make some comments on the relevance of the “adiabatic” approximation and the “temperature model” to experiments. In the experiments we are interested in, the equilibration of the electrons takes place in subpicosecond time scale while the time scale for energy loss to the lattice is picoseconds, indicating that the adiabatic approximation is reasonable. There is also experimental evidence in favor of the temperature model. The experimental luminescence profile, which directly measures the distribution function, yields a Fermi-like distribution in the tail and is used to determine the effective temperature of the excited electrons. In steady-state transport experiments the situation is somewhat more complicated because the electrons continuously gain energy from the applied electric field and lose it to the lattice, but here also luminescence spectrum shows that the electron distribution is to a good approximation thermal. In the rest of the paper we will assume that the electrons are in internal equilibrium and can be described by an effective electron temperature which is higher than the lattice temperature. Even though this model has a limited applicability, it is very useful because of its simplicity and concreteness, allowing one to perform detailed calculations and to compare them with appropriate experimental situations. It also facilitates identification and study of physical phe-

phenomena. In the experiments we are interested in, the equilibration of the electrons takes place in subpicosecond time scale while the time scale for energy loss to the lattice is picoseconds, indicating that the adiabatic approximation is reasonable. There is also experimental evidence in favor of the temperature model. The experimental luminescence profile, which directly measures the distribution function, yields a Fermi-like distribution in the tail and is used to determine the effective temperature of the excited electrons. In steady-state transport experiments the situation is somewhat more complicated because the electrons continuously gain energy from the applied electric field and lose it to the lattice, but here also luminescence spectrum shows that the electron distribution is to a good approximation thermal. In the rest of the paper we will assume that the electrons are in internal equilibrium and can be described by an effective electron temperature which is higher than the lattice temperature. Even though this model has a limited applicability, it is very useful because of its simplicity and concreteness, allowing one to perform detailed calculations and to compare them with appropriate experimental situations. It also facilitates identification and study of physical phe-

nomena important in the physics of hot-carrier relaxation. The electron-temperature model is valid for the experimental situations with which we compare our theoretical results in this paper.

The laser-pulse-excitation experiments produce electron temperature as a function of time, while the steady-state electric-field-heating experiments produce power loss as a function of electron temperature. In the bulk of this paper we will calculate power loss as a function of electron temperature since it is the natural quantity to compute theoretically, but we will also discuss how to obtain the electron temperature as a function of time using our results.

In this work we restrict ourselves to electrons near the bottom of the conduction band and assume effective-mass approximation and parabolic bands. We will also consider only the situation in which there are no holes created in the valence band. This assumption is not necessarily valid when the electrons are excited in an undoped semiconductor by a laser pulse, but is reasonable for steady-state electric-field-heating experiments in doped semiconductors. The holes in the valence band can be treated in a manner analogous to the one sketched out for electrons in this paper, but here we do not want to complicate the issues we are interested in by including the complexity of the hole band structure. We will consider three-dimensional semiconductor systems as well as two-dimensional semiconductor quantum wells where the bulk of the recent experimental interest lies. Due to the effective-mass approximation, our calculations are applicable to wide-band-gap systems such as the conduction-band electrons in InP, GaP, and GaAs, and we will use parameters appropriate for GaAs in this paper. A short report of parts of this paper has been published.⁴

We will mostly consider hot-electron-energy loss via LO-phonon emission. Since coupling of the electrons to acoustic phonons is much weaker, LO phonons dominate the energy-loss process except at very low temperatures. Consider now the steady-state electric-field-heating experiments. The energy loss occurs in four steps: (i) the electrons gain energy from the electric field, (ii) they lose energy by emitting LO phonons, (iii) LO phonons decay into acoustic phonons via anharmonic processes, and finally (iv) the lattice thermalizes with the surrounding liquid-helium bath. Because LO phonons have a finite lifetime [$\tau_{\text{ph}} \approx 7$ ps in GaAs (Ref. 5)], there is finite probability of their being reabsorbed by the electrons, which effectively reduces the power loss and, thus, has to be explicitly taken into account. In fact, the power loss is really decided by *how many LO phonons decay per second*; if LO phonons had an infinite lifetime, there would be no power loss—the number of LO phonons present in the system would simply stabilize where the phonon emission and the phonon reabsorption rates are equal. We emphasize again that energy redistribution among the individual electrons themselves (e.g., emission of a plasmon) does not cause any power loss for the whole electron gas, and power loss can occur only via phonon emission.

We have already indicated one important piece of the hot-electron-relaxation physics, namely, phonon reabsorption, or, as it is often called in the literature, the

“hot-phonon effect.”⁶ There are several other effects that must be included in any theoretical calculation because of their quantitative importance. The electron-electron interaction screens^{7–9} and generally weakens the electron-phonon coupling, thus reducing the power loss. This gives power loss a density dependence, since the effectiveness of screening is a strong function of the electron density. The LO phonons are themselves renormalized by the presence of the electron gas, of which plasmon-phonon mode coupling⁹ is a well known example. This renormalization creates new low-energy phonon modes into which the electrons can lose their energy, and even though the oscillator strength of these new modes is exceedingly small, we will show that they make an important correction in the power loss at low electron temperatures. In the case of a quantum well, the LO phonons as well as the electrons are confined within the quantum well, and a careful treatment of this confinement is necessary to determine the electron-phonon coupling.¹⁰ The electron-electron interaction and the electron-phonon coupling depend also on the width of the quantum well, and in what follows we will also discuss the width dependence of the power loss in detail.

We will consider temperatures low enough ($k_B T \ll \hbar\omega_{\text{LO}}$) so that only the one-phonon emission process is significant. For GaAs, for which $\hbar\omega_{\text{LO}} = 36$ meV, this implies a temperature below 300–400 K. The situation is shown schematically in Fig. 1. One can deduce the important temperature dependence of the power loss by noticing that only the electrons with energy higher than $\hbar\omega_{\text{LO}}$ are capable of emitting a LO phonon. These electrons are usually in the high-energy tail of the Fermi distribution and the power loss is proportional to their

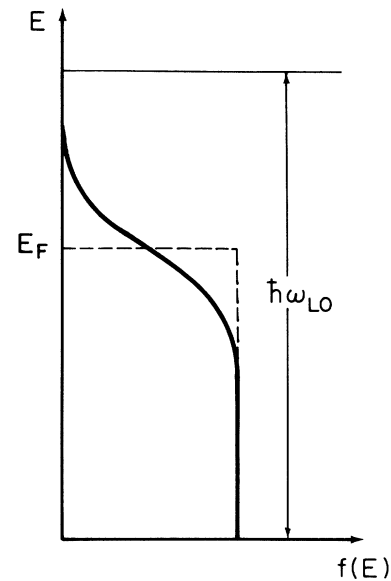


FIG. 1. Fermi distribution $f(E)$ as a function of the electron energy E . The electrons capable of emitting LO phonon are those with energies E above $\hbar\omega_{\text{LO}}$.

number, which in turn is proportional to the exponential factor $\exp(-\hbar\omega_{\text{LO}}/kT)$:

$$P = \frac{\hbar\omega_{\text{LO}}}{\tau} e^{-\hbar\omega_{\text{LO}}/k_B T}. \quad (1)$$

The prefactor $\hbar\omega_{\text{LO}}/\tau$ is introduced for dimensional reasons. The energy relaxation time τ , can be calculated from first principles and is expected to be only weakly temperature dependent. Therefore, the main temperature dependence of the power loss is given by the exponential factor. Equation (1) is valid only for power loss to bare phonons; as mentioned earlier, phonon renormalization provides new low-energy modes which invalidate the reasoning leading to Eq. (1). In the presence of these low-energy modes, a simple equation like Eq. (1) cannot be written down to describe the power loss, and one must use detailed many-body theory for its evaluation. We will see in the course of this paper that various formulas for power loss reduce to this simple equation in the appropriate limits.

It should be emphasized that Eq. (1) has been the basis for interpreting hot-electron energy-loss experiments for about 25 years.¹¹ Usually τ is calculated from the electron-phonon scattering rate using Fermi's golden rule (cf. Sec. II). Recently, a number of papers⁷⁻⁹ have appeared in the literature incorporating screening and hot-phonon effects in the power-loss calculations. We have recently published⁹ results of our power-loss calculations both in two- and three-dimensional systems including effects of quantum degeneracy (Fermi statistics), dynamical screening, hot-phonon effects, and plasmon-phonon coupling effects. In the current paper we provide a complete theory [within the electron-temperature model and using the random-phase approximation (RPA)] for hot-electron energy loss via optical-phonon emission in a weakly polar material by including full effects of phonon self-energy correction. A detailed comparison of quantitative corrections induced by various effects (e.g., degeneracy, screening, hot-phonon effects, etc.) has already been provided in our earlier work⁹ and will not be repeated here.

The plan of the paper is as follows. Section II contains the basic theoretical formalism. Sections III and IV deal with the hot-electron effect and the phonon self-energy correction. In Secs. V and VI we give the results of our calculation for three- and two-dimensional systems, respectively. In Sec. VII we briefly describe the effects of slab phonon modes in quantum wells and in Sec. VIII we point out how to obtain time-dependent energy loss from our theoretical results. We conclude in Sec. IX.

II. THEORY

As explained in the Introduction, we wish to study a quasiequilibrium situation in which the electrons and the lattice are separately in equilibrium, coupled only weakly through electron-phonon interaction. We assume that the electron distribution function can be described by an effective temperature T which is higher than the lattice temperature T_L . We wish to calculate the rate at which

the electrons lose energy to the lattice excitations. The standard method for doing this, which has also been mistakenly applied to this problem, is to calculate the electron self-energy, $\Sigma(k, \epsilon)$, whose imaginary part is then simply related to the electron relaxation rate. This approach is, however, not valid here. We are considering here a nonequilibrium process with the electrons and phonons at different temperatures, whereas the standard expressions for $\Sigma(k, \epsilon)$, derived from an equilibrium-field-theory approach, assume the same temperature for both. Moreover, $\text{Im}\Sigma(k, \epsilon)$ yields the relaxation rate for a single electron with momentum and energy k and ϵ , respectively, whereas we are interested in the energy-loss rate of the *whole* electron gas. We will make further comments on this issue later in this section.

The correct way to calculate the power loss is simply to use Fermi's "golden rule." Before we use Fermi's golden rule for the general situation, we start by reviewing a rather simplified, but very instructive model, which contains many of the essential features of the complete result. This model considers noninteracting electrons obeying Maxwell-Boltzmann statistics. It will not only serve to define our notation, but also form an intuitive basis for understanding the more complicated models to be considered later. The total power loss is given (setting $\hbar=1$ from now on) by

$$P = \int_{\omega_{\text{LO}}}^{\infty} dE g(E) P(E) e^{-E/k_B T}, \quad (2)$$

where $g(E)$ is the electronic density of states and $P(E)$ is the power loss of an electron with energy E given by Fermi's golden rule,

$$P(E_k) = 2\pi \sum_{\mathbf{q}} \omega_{\text{LO}} M_q^2 \delta(E_{\mathbf{k}-\mathbf{q},f} - E_{\mathbf{k},i} + \omega_{\text{LO}}), \quad (3)$$

where ω_{LO} is the LO-phonon energy (assumed to be dispersionless), i and f are the initial and the final electronic states, and the sum is over the phonon wave vector \mathbf{q} , assumed to have the same dimensionality as the electrons [three dimensional (3D) for bulk semiconductors and 2D for quantum wells]. M_q is the electron-phonon matrix element¹² given by

$$M_q^2 = \begin{cases} \frac{4\pi\alpha(\omega_{\text{LO}})^{3/2}}{\sqrt{2m}} \frac{1}{q^2} & \text{in 3D,} \\ \frac{2\pi\alpha(\omega_{\text{LO}})^{3/2}}{\sqrt{2m}} \frac{1}{q} & \text{in 2D,} \end{cases} \quad (4a)$$

$$M_q^2 = \begin{cases} \frac{4\pi\alpha(\omega_{\text{LO}})^{3/2}}{\sqrt{2m}} \frac{1}{q^2} & \text{in 3D,} \\ \frac{2\pi\alpha(\omega_{\text{LO}})^{3/2}}{\sqrt{2m}} \frac{1}{q} & \text{in 2D,} \end{cases} \quad (4b)$$

where $\alpha = e^2 \sqrt{m/2\omega_{\text{LO}}} (1/\epsilon_{\infty} - 1/\epsilon_0)$ is the dimensionless polaron coupling constant. In the 2D case we are assuming that the confined electrons interact with dispersionless bulk phonons. More realistic models modify the matrix element of (4b) and will be studied later in this paper. Notice that during the phonon-emission process the Pauli principle, which requires that the transition be possible only if the final state is unoccupied, has been ignored. In Eq. (2), because the lower limit of the energy integral is ω_{LO} , we expect a factor $\exp(-\omega_{\text{LO}}/k_B T)$ in the expression for power loss. Fortunately, this integral can be explicitly evaluated and one obtains Eq. (1) with

$$\tau_{3D} = (2\alpha\omega_{LO})^{-1} \quad (5a)$$

and

$$\tau_{2D} = (\pi\alpha\omega_{LO})^{-1}. \quad (5b)$$

The numerical values for GaAs from this simple theory are $\tau_{3D} = 0.13$ ps and $\tau_{2D} = 0.08$ ps.

This simple model is expected to be valid for a low-density electron gas with $k_B T \gg E_F$ since Maxwell-Boltzmann statistics have been used and electron-electron interaction has been ignored. For general values of parameters, the observed relaxation times are different from Eqs. (5), suggesting the need for an improved model. However, even this simple model provides a qualitatively correct description of experiments at relatively high temperatures in that it predicts the observed linear slope of $-\omega_{LO}/k_B$ for the curve of $\ln P$ versus $1/T$. As we argued earlier, this result is much more general than suggested by this simple model and holds so long as one ignores phonon renormalization and considers power loss only to bare phonons.

For completeness, we now sketch a derivation of the Kogan formula¹¹ for power loss, which is a simple application of Fermi's golden rule to the many-body system consisting of electrons, the lattice, and the interaction between them. We generalize the Kogan formula slightly to suit our purpose of later including phonon self-energy correction. The many-body Hamiltonian is given by

$$H = H_0 + H_1, \quad (6)$$

$$H_0 = \sum_{\mathbf{k}} \omega_{\mathbf{k}} b_{\mathbf{k}}^\dagger b_{\mathbf{k}} + \sum_{\mathbf{k}} \epsilon_{\mathbf{k}} c_{\mathbf{k}}^\dagger c_{\mathbf{k}} + \frac{1}{2V} \sum_{\mathbf{q}} V_{\mathbf{q}} \rho_{\mathbf{q}} \rho_{-\mathbf{q}}, \quad (7a)$$

$$H_1 = \frac{1}{\sqrt{V}} \sum_{\mathbf{q}} (M_{\mathbf{q}} \rho_{-\mathbf{q}} b_{\mathbf{q}} + M_{\mathbf{q}}^* \rho_{\mathbf{q}} b_{\mathbf{q}}^\dagger), \quad (7b)$$

where b^\dagger and b are creation and annihilation operators for phonons, c^\dagger and c are the creation and annihilation operators for electrons, $V_{\mathbf{q}}$ is the Coulomb matrix element, $M_{\mathbf{q}}$ is the Fröhlich matrix element given by Eqs. (4), V is the volume of the system, $\omega_{\mathbf{k}}$ and $\epsilon_{\mathbf{k}}$ are the phonon and electron energies, and $\rho_{\mathbf{q}}$ is the Fourier transform of the electron density operator:

$$\rho_{\mathbf{q}} = \sum_{\mathbf{k}} c_{\mathbf{k}-\mathbf{q}}^\dagger c_{\mathbf{k}}. \quad (8)$$

We will treat the electron-phonon interaction Hamiltonian H_1 as a perturbation to H_0 . The emission rate from the initial many-body state $|i, \{N_{\mathbf{q}}\}_i\rangle$ to the final many-body state $|f, \{N_{\mathbf{q}}\}_f\rangle$ by emitting a phonon of wave vector \mathbf{q} is given by

$$W_{em}(\mathbf{q}) = \sum_{i,f} 2\pi \hat{w}_i |\langle f, \{N_{\mathbf{q}}\}_f | H_1 | i, \{N_{\mathbf{q}}\}_i \rangle|^2 \times A(E_i - E_f), \quad (9)$$

where i and f correspond to electronic states, $\{N_{\mathbf{q}}\}_i$ and $\{N_{\mathbf{q}}\}_f$ are the set of phonon occupation numbers for the initial and final states (differing only by $N_{\mathbf{q},f} = N_{\mathbf{q},i} + 1$ in

the process of emission of a phonon with wave vector \mathbf{q}), $A(\omega)$ is the phonon density of states, and \hat{w}_i is the weighting factor for the initial many-body electronic state. Substituting H_1 from Eqs. (7) and performing the ensemble average over the initial lattice states, we obtain the following phonon-emission rate:

$$W_{em}(\mathbf{q}) = \frac{1}{V} \sum_{i,f} 2\pi \hat{w}_i |\langle f | \rho_{-\mathbf{q}} | i \rangle|^2 M_{\mathbf{q}}^2 (N_{\mathbf{q}} + 1) A(E_i - E_f). \quad (10)$$

Similarly the absorption rate is given by

$$W_{ab}(\mathbf{q}) = \frac{1}{V} \sum_{i,f} 2\pi \hat{w}_i |\langle f | \rho_{-\mathbf{q}} | i \rangle|^2 M_{\mathbf{q}}^2 N_{\mathbf{q}} A(E_f - E_i). \quad (11)$$

Assuming a thermal distribution at the lattice temperature T_L for the phonons, the average value of the occupation numbers is given by the Bose factor $N_{\mathbf{q}} = [\exp(\omega_{\mathbf{q}}/k_B T_L) - 1]^{-1}$. The power loss is then given by

$$P = \sum_{\mathbf{q}} \omega_{\mathbf{q}} [W_{em}(\mathbf{q}) - W_{ab}(\mathbf{q})] \\ = \frac{1}{V} \sum_{\mathbf{q}} \int d\omega \omega (N_{\mathbf{q}} + 1 - e^{\omega/k_B T} N_{\mathbf{q}}) M_{\mathbf{q}}^2 A(\omega) \\ \times \left[\sum_{i,f} 2\pi \hat{w}_i |\langle f | \rho_{\mathbf{q}} | i \rangle|^2 \delta(E_i - E_f - \omega) \right]. \quad (12)$$

In obtaining (12), one first makes the exchange $i \leftrightarrow f$ in (11) and then uses $\hat{w}_f = \exp[(E_i - E_f)/k_B T] \hat{w}_i$. The quantity in the square brackets is the time Fourier transform of the correlation function $\langle \rho_{-\mathbf{q}}(0) \rho_{\mathbf{q}}(t) \rangle$, which is related to the standard retarded density-correlation function, $\Pi(q, \omega)$ (the "bubble") by the Callen-Welton-Kubo fluctuation-dissipation theorem in the following way:

$$\int dt e^{i\omega t} \langle \rho_{-\mathbf{q}}(0) \rho_{\mathbf{q}}(t) \rangle = -2V n_T(\omega) \text{Im} \Pi(q, \omega). \quad (13)$$

$n_T(\omega)$ is the Bose factor at the electron temperature, and the time-dependent operator $\rho_{\mathbf{q}}(t)$ is expressed in the interaction representation. The final expression for power loss is

$$P = \sum_{\mathbf{q}} \int \frac{d\omega}{\pi} \omega M_{\mathbf{q}}^2 [n_{T_L}(\omega) - n_T(\omega)] \\ \times \text{Im} \Pi(q, \omega) \text{Im} D(q, \omega). \quad (14)$$

We have used the fact that the phonon density of states is given by $A(q, \omega) = -\pi^{-1} \text{Im} D(q, \omega)$, where D is the phonon propagator. We should point out that for the interacting system, we could imagine working with a renormalized Hamiltonian where H_1 contains the renormalized phonon operators. This heuristic argument leads to Eq. (14) with D as the renormalized phonon propagator. We will take $T_L = 0$, unless mentioned otherwise, and drop the $n_{T_L}(\omega)$ term, which is equivalent to ignoring phonon absorption. Several comments are now in order.

As is clear from the way Fermi's golden rule has been applied, $\text{Im}\Pi(q, \omega)$ is entirely an electronic quantity and must include only electron-electron interaction and no electron-phonon interaction. The formula (14) explicitly contains the phonon density of states through $\text{Im}D$, and therefore, it is easy to incorporate phonon renormalization (or phonon self-energy correction) in the calculation. For bare phonons, D is replaced by D^0 ,

$$D^0(q, \omega) = \frac{2\omega_{\text{LO}}}{\omega^2 - \omega_{\text{LO}}^2}, \quad (15)$$

and $\text{Im}D^0(q, \omega) = -\pi[\delta(\omega - \omega_{\text{LO}}) - \delta(\omega + \omega_{\text{LO}})]$, leading to

$$P_{\text{bare}} = \omega_{\text{LO}} n_T(\omega_{\text{LO}}) \left[-2 \sum_q M_q^2 \text{Im}\Pi(q, \omega_{\text{LO}}) \right] \quad (16)$$

For $k_B T \ll \omega_{\text{LO}}$, $n_T(\omega_{\text{LO}}) \simeq \exp(-\omega_{\text{LO}}/k_B T)$, and thus one has obtained an explicit formula for the electron relaxation time τ defined in Eq. (1). We have numerically checked that for low densities and no screening (i.e., no Coulomb interaction) one recovers $\tau_{3\text{D}} \simeq 0.13$ ps and,

$$\Pi_0(q, \omega) = \begin{cases} -\frac{3}{8} \frac{n}{E_F} \frac{k_F}{q} [H(a_+) - H(a_-)] & \text{for 3D} \\ -\frac{n}{E_F} \frac{k_F}{q} \left[\frac{q}{k_F} - (a_+^2 - 1)^{1/2} + (a_-^2 - 1)^{1/2} \right] & \text{for 2D,} \end{cases} \quad (20a)$$

$$\quad (20b)$$

where

$$a_{\pm} = \frac{\omega + i\gamma}{qv_F} \pm \frac{q}{2k_F},$$

and

$$H(z) = 2z + (1 - z^2) \ln \left[\frac{z+1}{z-1} \right].$$

The logarithm is taken from the branch where $|\text{Im} \ln z| < \pi$, and the complex square root is chosen to be on the branch with positive imaginary part. In Eqs. (20) the finite value of γ takes into account the electron scattering by impurities phenomenologically. We have also used in our numerical calculations the particle-conserving formula for the dielectric function in the presence of impurity scattering suggested¹⁴ by Mermin and obtained essentially the same results as those obtained using Eqs. (20) directly. The finite temperature $\Pi_0(q, \omega; T, \mu)$ can be obtained¹⁵ using the formula

$$\Pi_0(q, \omega; T, \mu) = \int_0^\infty \frac{\Pi_0(q, \omega; T=0, \mu')}{4k_B T \cosh^2[(\mu - \mu')/2k_B T]} d\mu'. \quad (21)$$

At zero temperature, $\text{Im}\Pi_0(q, \omega; T=0)$ is nonzero only in the single-particle excitation region defined by

$$E_k - E_{k+q} = \omega. \quad (22)$$

$\tau_{2\text{D}} \simeq 0.08$ ps obtained earlier analytically in a simplified model. This again illustrates that the simple expression for power loss in Eq. (1) is valid (with τ treated as a fitting parameter) as long as only the power loss to bare LO phonons is considered.

In contrast to the simple theory, Eq. (14) for power loss contains the effects of electron-electron interaction through the retarded polarizability function, which in the Bohm-Pines random-phase approximation¹³ is given by

$$\Pi(q, \omega) = \frac{\Pi_0(q, \omega)}{\epsilon(q, \omega)}, \quad (17)$$

$$\Pi_0(q, \omega) = -2 \sum_p \frac{f(E_{p+q}) - f(E_p)}{\omega + i\gamma - E_{p+q} + E_p}, \quad (18)$$

$$\epsilon(q, \omega) = 1 - V_q \Pi_0(q, \omega), \quad (19)$$

where Π_0 is the irreducible polarizability, $f(E_p)$ is the Fermi occupation factor at energy $E_p = p^2/2m$, and ϵ is the electronic dielectric function. At zero temperature, Π_0 , the Lindhard function, is given by the bare "bubble" diagram

Thus, only bare LO phonons of large wave vectors can be emitted. At finite temperatures contribution to the q integral in Eq. (16) in principle comes from all wave vectors, but at low temperatures the dominant contribution is still expected to come from the region inside the *zero-temperature* single-particle excitation region.

Several approximations for $\epsilon(q, \omega_{\text{LO}})$ appearing in Eq. (17) have been used in the literature. The "no-screening approximation" ($\epsilon = 1$) is expected to be valid at low electron densities when screening is unimportant. On the other hand, the "static-screening approximation" [$\epsilon = \epsilon(q, \omega = 0)$] is expected to be appropriate for large densities, because then ω_{LO} is very small compared to the typical energy associated with the electrons, namely, the plasma energy ω_p . With our numerical calculations we have explicitly verified these intuitive expectations. Details of these calculations have been given in Ref. 9 and will not be repeated here. In the numerical calculations presented in this paper we will always use the complete dynamical $\epsilon(q, \omega)$ obtained in the RPA.

III. HOT-PHONON EFFECT

The formula (14) for power loss is correct only if the LO phonons created during electronic transitions to lower energies decay instantaneously through anharmonic processes into acoustic phonons which then immediately thermalize with the surrounding bath. Practically, however, this is not the case since the LO phonons have a finite lifetime τ_{ph} before they decay into acoustic pho-

nons. Therefore, there is a finite probability of the LO phonons being reabsorbed by the electron gas, which would result in a power gain, and a net power loss lower than that predicted by Eq. (14) [or Eq. (16)]. This effect has been studied in great detail for bare LO phonons and can be included phenomenologically quite accurately in the following manner. The rate of change of the phonon occupation number $N(q, \omega)$ is given by

$$\frac{dN(q, \omega)}{dt} = R_{em}[N(q, \omega) + 1] - R_{ab}N(q, \omega) - \frac{N(q, \omega)}{\tau_{ph}(\omega)} \quad (23)$$

which must be zero in the steady state. Here $\tau_{ph}(\omega)$ is the lifetime of the phonon of energy ω ; R_{em} and R_{ab} are the emission and absorption rates, respectively, related by $R_{ab} = e^{\omega/k_B T} R_{em}$ according to the principle of detailed balance. The last term in Eq. (23) explicitly takes into account the decay of LO phonons into acoustic modes. The dissipated power, which is proportional to the number of phonons decaying per unit time, is given by

$$P = \sum_q \int d\omega \omega \frac{N(q, \omega)}{\tau(\omega)} = \sum_q \int d\omega \omega \frac{R(q, \omega)}{1 + \tau(\omega)R(q, \omega)} n_T(\omega), \quad (24)$$

where $R(q, \omega) = R_{em}(q, \omega)/n_T(q, \omega)$. Thus, in order to include the hot-phonon effect, one first writes Eq. (14) as

$$P = \sum_q \int d\omega \omega R(q, \omega) n_T(\omega) \quad (25)$$

which is nothing but Eq. (24) with $\tau(\omega) = 0$ and merely serves to define $R(q, \omega)$. In the presence of hot phonons one then replaces $R(q, \omega)$ in the integrand by $R(q, \omega)[1 + \tau(\omega)R(q, \omega)]^{-1}$. We consider here only the special case of bare LO phonons, in which Eq. (14) reduces to Eq. (16). The power loss including the hot-phonon effect is then given by

$$P = \omega_{LO} n_T(\omega_{LO}) \sum_q \frac{R(q, \omega_{LO})}{1 + \tau_{ph} R(q, \omega_{LO})} \quad (26)$$

with

$$R(q, \omega_{LO}) = -2M_q^2 \text{Im}\Pi(q, \omega_{LO}). \quad (27)$$

In Fig. 2 we show $\log_{10}(P)$ as a function of T^{-1} for various values of τ_{ph} . For $\tau_{ph} = 7$ ps, the power loss is reduced by approximately an order of magnitude, and explains quite well the available 2D experimental data^{16,17} at high electron temperatures. Note that the hot-phonon effect is of quantitative significance only when $\tau_{ph} \gg \tau$.

Notice that the plot of $\log_{10}(P)$ as a function of T^{-1} is approximately a straight line, which is consistent with Eq. (1) and is quite generally true for power loss to bare LO phonons in the temperature range $k_B T \ll \omega_{LO}$. This can be seen immediately in Eq. (16) or in the corresponding hot-phonon effect including Eq. (26) where the power loss also is proportional to $n_T(\omega_{LO})$ which can be approximated by $n_T(\omega_{LO}) \sim \exp(-\omega_{LO}/k_B T)$ for $k_B T \ll \omega_{LO}$.

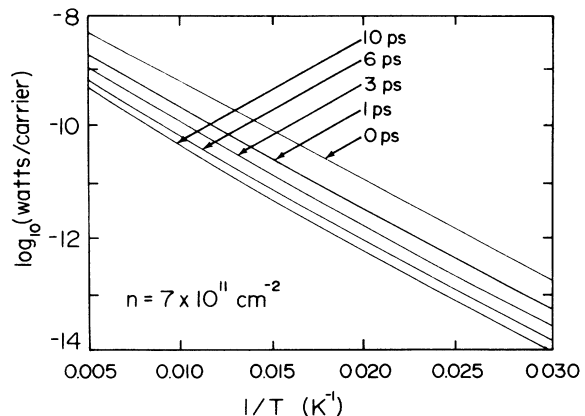


FIG. 2. Power loss as a function of the inverse electron temperature for several values of the phonon lifetime τ_{ph} .

The other factors in the expression for the power loss are also temperature dependent, but only weakly so, and the dominant temperature dependence comes from the exponential term $\exp(-\omega_{LO}/k_B T)$. Thus, so long as one considers only bare LO phonons, different approximations (no screening, dynamic screening, static screening, hot-phonon effect, etc.) only rigidly shift the nearly straight line in the plot of $\log_{10}(P)$ versus T^{-1} . Experimentally, a straight line is observed only at relatively high temperatures, and there is considerable bending (towards higher power loss) at low temperatures. This bending is usually attributed uncritically to acoustic phonons, even though there has not been any serious successful attempt at a quantitative comparison between theory and experiment. In some isolated cases the power loss obtained from theoretical calculations including acoustic phonons was found to underestimate the power loss observed experimentally, and one finds mention of “missing” energy-loss channels in the literature. We have shown⁴ that certain subtle many-body corrections give rise to novel channels into which the electrons can dissipate energy. These channels dominate the power-loss process under certain conditions and produce a bending in the plot of $\log_{10}(P)$ versus T^{-1} in the correct direction. We have been able to obtain a reasonable agreement with experiments down to fairly low temperatures without recourse to acoustic phonons. In this paper our emphasis will be on understanding these lower-temperature energy-loss processes—the situation for higher temperatures has been discussed in details in our earlier publications⁹ and our current results are very similar to these published results for higher electron temperatures.

In the next section we discuss these extra phonon modes, which show up in the renormalized LO-phonon density of states (or spectral function) and dominate energy relaxation at low enough temperatures.

IV. PHONON SPECTRAL FUNCTION

As mentioned before, the spectral function for the bare LO phonon is given by

$$A(q, \omega) = -\pi^{-1} \text{Im} D^0(q, \omega) = \delta(\omega - \omega_{LO}) - \delta(\omega + \omega_{LO}) \tag{28}$$

and has vanishing weight everywhere except at the bare-phonon energy. This is, however, not true for a LO phonon coupled to an electron gas, in which case the renormalized phonon spectral function has finite weight at other energies also. A well-known example of this is the plasmon-phonon mode coupling phenomenon. Since it plays a crucial role in the physics of hot-electron relaxation under certain conditions (to be elaborated on later), we consider the phonon renormalization in detail here. Following the usual procedure,¹⁸ we renormalize the phonon propagator by summing up the ring diagrams (Fig. 3), which lead to

$$D(q, \omega) = \frac{2\omega_{LO}}{\omega^2 - \omega_{LO}^2 - 2\omega_{LO} M_q^2 \Pi(q, \omega)} \tag{29}$$

The standard procedure is then to make what is known as the plasmon-pole or single-mode approximation for $\text{Im}\Pi(q, \omega)$. This approximation consists of ignoring the weight in the single-particle-excitation region and assuming that all the weight of $\text{Im}\Pi(q, \omega)$ lies at an “effective” plasmon energy. This is quite accurate in three dimensions at low wave vectors, and can be shown to be exact for $q=0$. The phonon spectral function can then be evaluated in a straightforward manner and has two delta-function peaks: one near the original phonon energy ω_{LO} , and the other near the plasmon energy ω_p . This phenomenon of plasmon-phonon coupling has been observed experimentally, and the experimental energies of the coupled modes show a remarkable agreement with the simple plasmon-pole results. The peak near the plasmon energy has a very small weight away from the mode-coupling region and therefore can be experimentally observed only near the mode-coupling region when the plasmon energy is close to the phonon energy.

In Fig. 4 we show the renormalized phonon spectral function calculated in the RPA, i.e., without making the usual plasmon-pole approximation. In addition to the weight at the plasmon and the bare-phonon energies, there is also some weight in the *single*-quasiparticle-excitation region, $\omega \lesssim qv_F$. Thus, there are three

branches in the renormalized phonon spectrum: the bare-phonon-like, the plasmonlike, and the quasiparticle-excitation-like (QPE-like). The oscillator strength of the plasmonlike phonon is very small, and that of the QPE-like phonons is still much smaller. In fact, the QPE-like phonons are so weak and broad that, to the best of our knowledge, they have been completely ignored prior to our work due perhaps to the intuitive feeling that such miniscule spectral weights could not play a significant role in any physical phenomenon. However, we find that the QPE-like phonons dominate the hot-electron power-loss process at low electron tem-

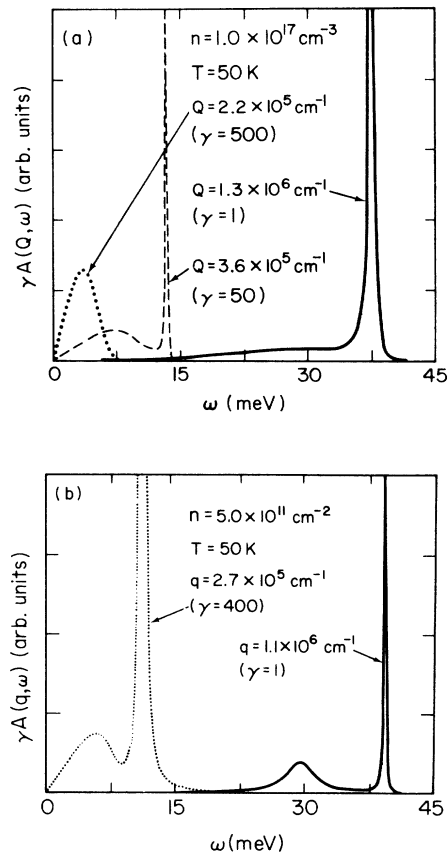


FIG. 4. (a) Phonon spectral function for three wave vectors in a 3D EG at an electron temperature of $T = 50$ K ($T_L = 0$). For $Q = 2.2 \times 10^5 \text{ cm}^{-1}$, the QPE branch extends from 0 to 7 meV, and there are δ -function peaks near the plasmon energy ($\omega_p \approx 14$ meV) and the phonon energy (36.8 meV) which are *not* shown explicitly in order to avoid too much detail. For $Q = 3.6 \times 10^5 \text{ cm}^{-1}$ the QPE branch extends up to ≈ 14 meV, and there is again a δ -function peak (not shown) at ω_{LO} . For $Q = 1.3 \times 10^6 \text{ cm}^{-1}$ the plasmonlike phonon is Landau damped, and the QPE-like phonons extend all the way up to ω_{LO} . The electron density is 10^{17} cm^{-3} , giving a Fermi vector of $1.4 \times 10^6 \text{ cm}^{-1}$. (b) Phonon spectral function for two wave vectors in a 2D EG. For $q = 2.7 \times 10^5 \text{ cm}^{-1}$ there is a δ -function peak (not shown) at ω_{LO} . The electron density is $5 \times 10^{11} \text{ cm}^{-2}$ giving a Fermi vector of $1.8 \times 10^6 \text{ cm}^{-1}$.

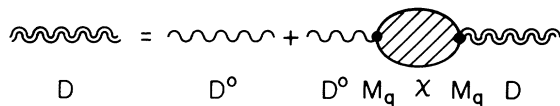


FIG. 3. Diagrammatic representation of Dyson's equation for the LO-phonon propagator. The bare propagator D^0 is represented by wiggly lines and the renormalized propagator D by double wiggly lines. The hatched bubble represents the reducible electronic polarizability χ , and the electron-phonon interaction M_q is represented by dots.

peratures. The underlying physics behind this apparently rather puzzling phenomenon is actually quite simple. The power loss to a phonon mode of energy ω is proportional to $M_q^2 A(q, \omega)$. This by itself would imply that the power loss via emission of the plasmonlike and QPE-like phonons would be negligible compared to the power loss via bare-LO-phonon emission. As indicated earlier, however, there is another competing effect that must also be taken into consideration. The power loss via emission of a phonon of energy ω is proportional to the number of electrons energetically capable of emitting a phonon of energy ω , which, in turn, is proportional to $\exp(-\omega/k_B T)$. This factor exponentially favors the lower-energy modes at low temperatures. Thus, it is clear that even though the low-energy modes (QPE-like phonons) have only a very small strength, they will always dominate over the high-energy modes (bare phonon) at low enough temperatures.

We want to mention a subtle (but quantitatively minor for the cases considered in this paper) theoretical point about our phonon renormalization correction. The diagrammatic expansion of Fig. 3 [or Eq. (29)] poses some ambiguity because our electron-phonon system is not in equilibrium (the electron and lattice temperatures are different). However, for the electron densities and temperatures considered in this work the reducible polarizability Π is a weak function of temperature, and we have checked numerically for several values of parameters that the calculated power loss is essentially independent of whether the Π appearing in Eq. (29) is evaluated at T , T_L , or an intermediate temperature. Therefore, even though the exact LO-phonon renormalization in the nonequilibrium situation is a very complicated problem which will not be addressed in this work, our approach will be to approximate it by the LO-phonon self-energy correction at the electron temperature T .

In addition to the QPE-like LO phonons, there are also acoustic phonons at low energies into which the electron gas can directly dissipate energy. Which phonon is dominant at a given electron temperature can be determined only by detailed numerical investigations. In the next section we give results of our numerical calculations. In summary, we find that (i) at high temperatures ($T \gtrsim 50$ K) the "bare" LO phonons dominate the power loss, (ii) at intermediate temperatures ($20 < T \lesssim 50$ K) power is lost predominantly to the plasmonlike or QPE-like branch of the LO-phonon spectrum, and (iii) at still-lower temperatures ($T \lesssim 20$ K) the acoustic phonons become important. The temperature ranges quoted in parentheses are only typical values, and the actual crossover temperatures depend sensitively upon experimental parameters, in particular, the density of electrons. For example, we find that for $n = 10^{16} \text{ cm}^{-3}$ in three dimensions the QPE-like phonons remain the leading mechanism for power loss down to 2 K, and only below 2 K do the acoustic phonons become relevant.

In our subsequent numerical calculations we will often omit the hot-phonon effect because of three reasons. The first reason is that unlike the bare LO phonon, there is not much direct experimental information on the lifetimes of the plasmonlike and QPE-like modes. In any

case these lifetimes are expected to be strongly dependent on the wave vector and the energy of these modes. Therefore, the most natural first approximation is to ignore the hot-phonon effect. Secondly, the QPE-like LO phonons are very similar to acoustic phonons and are, therefore, expected to have very short lifetimes. Therefore, as is the case for acoustic phonons, one expects the hot-phonon corrections to be unimportant for QPE-like phonons also. Finally, the electron-energy relaxation times associated with these modes are quite long (i.e., $\tau \gg \tau_{\text{ph}}$) so that any hot-phonon effect is much less significant.

V. THREE-DIMENSIONAL SEMICONDUCTORS

First, we show the results of our numerical calculations for doped three-dimensional bulk GaAs semiconductors. In Fig. 5 we plot $\log_{10}(\text{watts/carrier})$ as a function of inverse temperature for three different densities both with and without including the phonon self-energy corrections. While for bare phonons the plot is a straight line, for the renormalized phonons there is a large enhancement of the power loss at low temperatures. In Fig. 6 we plot $I(\omega)$ defined by $P = \int d\omega I(\omega)$ at three different temperatures. As expected, at high temperatures all the power loss occurs to the bare mode, and phonon self-energy correction is unimportant. As the temperature is lowered, first the loss to plasmonlike branch of the LO phonon shows up, and at very low temperatures almost all the power loss occurs via emission of the QPE-like LO phonons. Thus, the subtle many-body effects giving rise to the QPE-like LO-phonon modes influence the power loss at low electron temperatures in a striking manner.

One also expects the acoustic phonons to be important

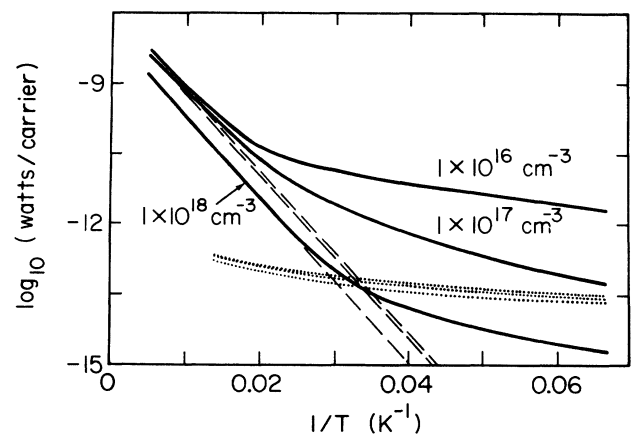


FIG. 5. Power loss as a function of the inverse electron temperature for a 3D EG (solid lines). The dashed lines correspond to power loss to bare LO phonons only. The dotted lines give the power loss to acoustic-phonon modes; the uppermost curve is for 10^{18} cm^{-3} , the middle one for 10^{16} cm^{-3} , and the lowest one for 10^{17} cm^{-3} . $T_L = 0$, and the power loss is expressed in watts per carrier.

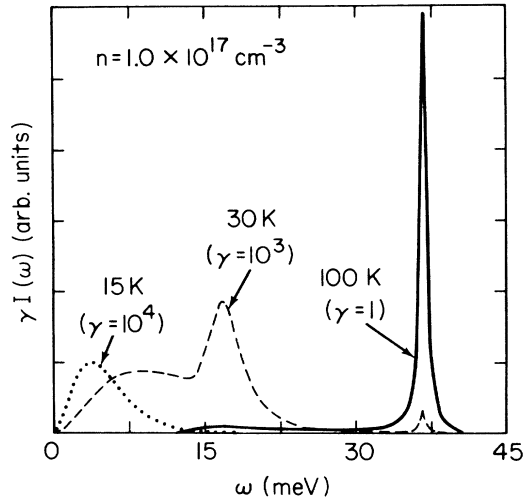


FIG. 6. Power-loss spectrum for a 3D EG with an electron density of 10^{17} cm^{-3} . At the electron temperature 100 K, the bare phonon dominates the power loss, while the QPE-like phonons dominate at 15 K.

at low electron temperatures. In order to investigate these modes vis-a-vis the QPE-like phonons, we also plot in Fig. 5 the calculated power loss to the acoustic phonons. While for the high-density electron-gas (EG) the acoustic phonons dominate below 30–40 K, for low densities the QPE-like LO-phonon modes dominate the power loss down to extremely low temperatures (down to 2 K for 10^{16} cm^{-3}).

VI. TWO-DIMENSIONAL SEMICONDUCTORS

Recently there has been a large amount of experimental work on hot-electron power loss in two-dimensional

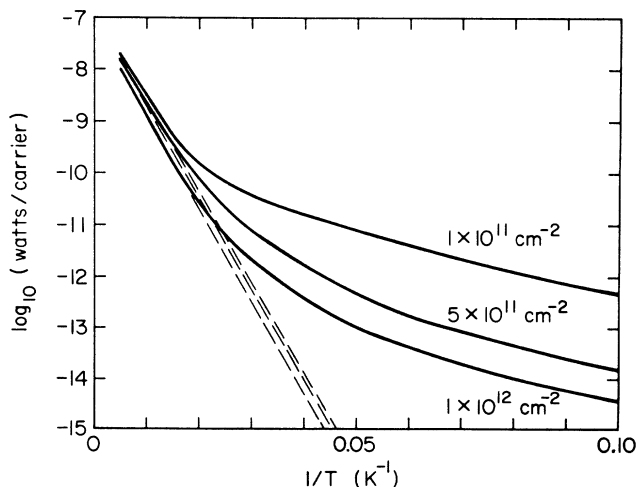


FIG. 7. Power loss as a function of the inverse electron temperature for a 2D EG (solid lines). The dashed lines correspond to power loss to bare LO phonons only. $T_L = 0$, and the power loss is expressed in watts per carrier.

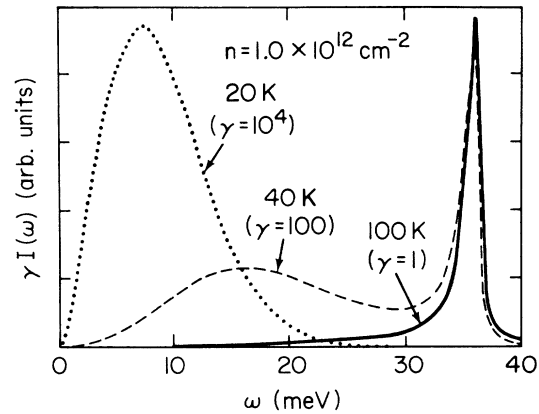


FIG. 8. Power-loss spectrum for a 2D EG with an electron density of 10^{12} cm^{-2} .

semiconductors (quantum wells and heterojunctions). Since our main interest is in the many-body effects, in order to keep the discussion as simple as possible, we will restrict ourselves in this section to the simple model described in Sec. III (strictly 2D electrons interacting with 3D phonons).

We show our numerical results (without including the hot-phonon effect) in Fig. 7 for three electron densities. The dashed lines show the power loss to only bare LO phonons. Clearly at high temperatures the power loss occurs predominantly through emission of bare LO phonons. At low electron temperatures the dashed lines underestimate the power loss by several orders of magnitude since the power loss is dominated by the QPE-like and plasmonlike phonons. This is seen very clearly in Fig. 8 where we plot the power-loss spectrum, $I(\omega)$, defined by $P = \int d\omega I(\omega)$. While at high temperatures all the power loss occurs essentially at ω_{LO} , at low temperatures the lower-energy modes dominate. Thus, inclusion of the low-energy modes leads to a large enhancement of power loss at low temperatures. In Fig. 8 the contributions from plasmonlike and QPE-like phonons do not show up separately because in two dimensions the plasmon energy is strongly wave-vector dependent.

VII. QUANTUM WELLS

In quantum wells (QW's) the real situation is more complicated than the simple model of the previous section due to finite-thickness effects. In order to make connections with experiments we must take into account the electron and phonon confinements. The finite thickness of the confining potential causes the electron wave functions to be spread over the well width and the appearance of different electronic subbands. Electrons can then lose energy either through intrasubband transitions or through intersubband transitions. For simplicity, we will assume in this paper that the electron densities are such that only the lowest subband is occupied and only the intrasubband transitions are allowed.

The phonon confinement and the electron-phonon coupling in QW's is not very well understood and is some-

what controversial. A simple approximation which is widely used (3D-phonon approximation) is to couple the quasi-2D electrons to the 3D phonons of the bulk. The 2D matrix element M_q of the electron-phonon interaction [Eq. (4b)] is then affected¹² by a subband form factor $f(q)$. This model, albeit simplistic, produces results which are qualitatively correct and quantitatively not too inaccurate when the well width is not very small ($> 80 \text{ \AA}$).

We have compared our calculated power loss within the 3D-phonon approximation with the experiments of Shah *et al.*¹⁶ and Yang *et al.*¹⁷ For the temperatures considered in these experiments (above 25 K) the QPE-like phonons and the acoustic phonons are not important, and we found reasonable agreement by including the bare and plasmonlike LO phonons.

A more realistic approach than the 3D-phonon approximation is to take into account the effects of the confining geometry in the LO-phonon spectrum by treating the QW as a thin film described by a long-wavelength lattice dielectric function. In this quasicontinuum model the presence of the QW gives rise to the bulklike confined slab modes and the interface slab modes (and consequently this is called the slab-phonon model). Both interface and bulk slab modes have been experimentally observed²⁰ via Raman scattering in thin quantum wells.

The simultaneous inclusion of the LO-phonon confining effects beyond the slab-phonon model and the phonon renormalization due to the electron gas is a very difficult problem which we will not address in this paper. However, Akera and Ando²¹ have recently shown that because of the large gap between the optical branches in the GaAs/AlAs case, the boundary conditions of zero parallel ion displacement at the interfaces used¹⁰ in the slab-phonon model are appropriate.

The power loss to the slab modes is still given by (14), with the appropriate matrix elements M_q . We have plotted in Fig. 9 the power loss per electron versus inverse electron temperature (for two QW thickness) showing the contributions of the bulk slab phonon and the symmetric interface phonon separately. The 3D-phonon-approximation (3D PA) result is also shown for comparison. The hot-electron effects are included in both approximations.

As in the previous models, in the high-temperature region, where the plot of $\log_{10}(P)$ versus $1/T$ is a straight line, the important contribution to power loss is coming from the bare LO phonon, and the phonon self-energy correction is unimportant. At low temperatures, deviation of the curve from the straight line signals the importance of phonon self-energy correction, and the plasmonlike and quasi-particle-like modes dominate the power loss. Here we want to emphasize the relative magnitudes of the various quantities shown in the plot. The 3D PA overestimates the power loss only by a small amount at high temperatures but by a factor of ~ 5 at low temperatures. The discrepancy at high temperatures would also be a factor of ~ 5 if one did not include the hot-phonon effect. The hot-phonon effect, which is significant only at high temperatures, makes the 3D PA results quite accurate because the power loss is largely controlled by the

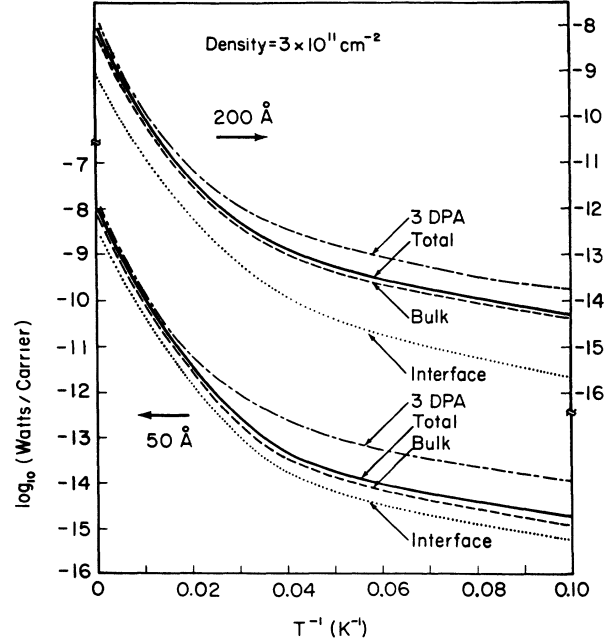


FIG. 9. Power loss as a function of inverse electron temperature for two QW's (widths 50 and 200 \AA) calculated in the 3D-phonon approximation and in the slab-phonon model. $T_L = 0$, and the power loss is expressed in watts per carrier.

relatively large phonon lifetime. Mathematically, the effective rate $1/(\tau + \tau_{ph})$ is not very sensitive to variations in τ for $\tau_{ph} \gg \tau$, which is usually the case since $\tau \leq 1$ ps and $\tau_{ph} \approx 7$ ps. In the trivial limit of $\tau_{ph} \rightarrow \infty$, the 3D PA result would be in exact agreement with the correct results. As expected, the bulk slab phonon dominates the power loss over the interface phonon, but for the thin QW the interface phonon also makes significant contribution.

VIII. TIME-DEPENDENT EXPERIMENTS

In the previous sections we have studied the power loss of hot electrons to LO phonons as occurring in a steady-state experiment (i.e., electric field heating).

For the time-dependent experiments²² (i.e., photoexcitation), there are two distinct regimes. During the first few femtoseconds (50–500 fs) following the excitation, the electron distribution is a highly nonequilibrium one, and the analysis used in the previous sections is not applicable at all. After this initial stage, luminescence measurements indicate that the electrons achieve a thermal distribution.

The fact that the electron temperature remains a well-defined quantity in the cooling process is a consequence of the smallness of the electron-equilibrium scattering time as compared with the electron-phonon relaxation time and allows us to use²³ the temperature model in the study of the time-dependent cooling. Within this quasi-static approach, the electron temperature T as a function of time t is given by the equation

$$\frac{dT}{dt} = -\frac{P(T)}{Nc_v(T)} \quad (30)$$

from an initial condition t_0, T_0 . In (30) N is the electron density, $c_v(T)$ is the electronic specific heat, and $P(T)$ is the power loss (whose temperature dependence has been calculated in the previous sections). One can integrate Eq. (30) starting from given initial conditions (t_0, T_0) to obtain $T \equiv T(t; t_0, T_0)$ using the results for $P(T)$ calculated in this paper.

IX. CONCLUSION

In this paper we have developed, within the electron-temperature model, a many-body theory for calculating the energy relaxation by hot electrons in a “cold” lattice. Specifically, we consider how the hot electrons lose their excess energy by emitting polar LO phonons in two- and three-dimensional GaAs systems. Our theory includes dynamical screening, quantum degeneracy, hot-phonon effects with the particular emphasis on the renormalization of the LO phonons by the excited electron gas itself. This last effect, a part of which is sometimes referred to as “the plasmon-phonon coupling” effect, also includes the many-body renormalization of LO phonons by elec-

tronic quasiparticles. We find that this quasiparticle renormalization of LO phonons gives rise to a novel decay channel for the excited electrons at low temperatures which could lead to orders-of-magnitude enhancement of the energy-loss rate (compared with the bare-LO-phonon case). We identify this novel process as the low-temperature “missing loss” mechanism which has been discussed in the literature.²⁴ Our theory for the two-dimensional quantum-well case includes the slab- and interface-phonon modes, showing a reduction in the energy-loss rates due to selection rules imposed by symmetry. Our results are in very good agreement with the available experimental data, even though more experiments at low electron temperatures are needed for a clear cut confirmation of our proposed novel power-loss mechanism.

ACKNOWLEDGMENTS

This work is supported by the United States Army Research Office (U.S. ARO) and the University of Maryland Computer Center. We would like to thank T. Kawamura for useful discussions and providing us with a version of Fig. 4(b).

-
- ¹J. Shah, J. Phys. (Paris) Colloq. **42**, C7-445 (1981).
²J. Shah, J. Quantum Electron. **QE-22**, 1728 (1986).
³S. A. Lyon, J. Lumin. **35**, 121 (1986).
⁴J. K. Jain, R. Jalabert, and S. Das Sarma, Phys. Rev. Lett. **60**, 353 (1988); **61**, 2005(E) (1988).
⁵J. A. Kash, J. C. Tsang, and J. M. Hvam, Phys. Rev. Lett. **54**, 2151 (1985); J. A. Kash, S. S. Jha, and J. C. Tsang, *ibid.* **58**, 1869 (1987).
⁶P. Kocevar, Physica B + C **134B**, 164 (1985); P. J. Price, *ibid.* **134B**, 155 (1985); S. M. Goodnick and P. Lugi, Phys. Rev. Lett. **59**, 716 (1987).
⁷J. R. Senna and S. Das Sarma, Solid State Commun. **64**, 1394 (1987); C. H. Yang and S. A. Lyon, Physica B + C **134B**, 309 (1985).
⁸W. Cai, M. C. Marchetti, and M. Lax, Phys. Rev. B **34**, 8573 (1986).
⁹S. Das Sarma, J. K. Jain, and R. Jalabert, Phys. Rev. B **37**, 1228 (1988); **37**, 4560 (1988); **37**, 6290 (1988); Solid-State Electron. **31**, 695 (1988).
¹⁰J. K. Jain and S. Das Sarma, Phys. Rev. Lett. **62**, 2305 (1989).
¹¹Sh. M. Kogan, Fiz. Tverd. Tela (Leningrad) **4**, 2474 (1963) [Sov. Phys.—Solid State **4**, 1813 (1963)]; E. Conwell, *High Field Transport in Solids* (Academic, New York, 1963).
¹²S. Das Sarma and B. A. Mason, Ann. Phys. (N.Y.) **163**, 78 (1985).
¹³See, for example, A. L. Fetter and J. D. Walecka, *Quantum Theory of Many-Particle Systems* (McGraw-Hill, New York, 1971).
¹⁴N. D. Mermin, Phys. Rev. B **1**, 2362 (1970).
¹⁵S. Das Sarma, Phys. Rev. B **33**, 5401 (1986); P. F. Maldague, Surf. Sci. **73**, 296 (1978).
¹⁶J. Shah, A. Pinczuk, A. C. Gossard, and W. Wiegmann, Phys. Rev. Lett. **54**, 2045 (1985).
¹⁷C. H. Yang, J. M. Carlson-Swindle, S. A. Lyon, and J. M. Worlock, Phys. Rev. Lett. **55**, 2359 (1985).
¹⁸See, for example, G. Mahan, *Many Particle Physics* (Plenum, New York, 1981).
¹⁹S. Das Sarma *et al.*, Phys. Rev. B **19**, 6397 (1979), and references therein.
²⁰A. K. Sood *et al.*, Phys. Rev. Lett. **54**, 2111, 2115 (1985).
²¹H. Akera and T. Ando, Phys. Rev. B **40**, 2914 (1989).
²²R. G. Ulbrich, Solid-State Electron. **21**, 51 (1978); D. J. Westland *et al.*, *ibid.* **31**, 431 (1988); K. Shum *et al.*, *ibid.* **31**, 451 (1988); M. Tatham *et al.*, *ibid.* **31**, 459 (1988).
²³J. Collet *et al.*, Solid State Commun. **42**, 883 (1982); R. P. Joshi and D. K. Ferry, Phys. Rev. B **39**, 1180 (1989).
²⁴D. J. Drummond *et al.*, Electron. Lett. **17**, 545 (1981); S. J. Manion *et al.*, Phys. Rev. B **35**, 9203 (1987); R. Ulbrich, *ibid.* **B 8**, 5719 (1973).